ELSEVIER

Ceramics International 33 (2007) 41–47

CERAMICS INTERNATIONAL

www.elsevier.com/locate/ceramint

Structural, dielectric and electrical studies in tungsten doped $SrBi_2Ta_2O_9$ ferroelectric ceramics

Indrani Coondoo [a], A.K. Jha [a,*], S.K. Agarwal [b]

[a] *Department of Applied Physics, Delhi College of Engineering, Bawana Road, Delhi 110042, India*
[b] *National Physical Laboratory, Dr. K.S. Krishnan Road, New Delhi 110012, India*

Received 7 April 2005; received in revised form 23 May 2005; accepted 8 July 2005
Available online 19 September 2005

Abstract

The effect of tungsten doping on the structural, dielectric and impedance properties of $SrBi_2Ta_2O_9$ (SBT) ferroelectric ceramics is reported. Tungsten doped $SrBi_2(W_xTa_{1-x})_2O_9$ ($0.0 \leq x \leq 0.20$) ceramics were synthesized by the solid state reaction method. X-ray diffractograms of the samples reveal the single phase layered perovskite structure formation with tungsten content $x \leq 0.05$. Variation in the lattice parameters has been explained in terms of the limited structural constraint and relaxation imposed by the Bi–O interlayer. Dielectric constant (ε) and dielectric loss (tan δ) measurements as a function of temperature reveal a decrease in the Curie temperature (T_c) from 320 °C (for $x = 0.0$) to 291 °C (for $x = 0.025$) and an increasing trend over the doping range of $0.05 \leq x \leq 0.20$. Significant reduction in the dielectric loss with tungsten addition have been observed. The observed changes in ε and tan δ with frequency and temperature have been considered in the light of oxygen and cationic vacancies in tungsten doped samples. Dielectric constant of the samples increases with tungsten doping at their respective Curie temperatures. These have been viewed in terms of relative dominance of the ionic and electronic polarizations. Bulk conductivity of the samples as deduced through ac impedance investigations indicate an increased electronic conduction beyond the observed solubility limit of 0.05 of tungsten doping.

Keywords: Dielectric properties; Impedance; Ferroelectric ceramics: solid state reaction; X-ray diffraction

1. Introduction

Ceramic materials having ferroelectric behaviour have found many applications in electronics and optics. A large number of ferroelectric ceramic devices exploit properties that are indirect consequence of ferroelectricity, viz. dielectric, piezoelectric, pyroelectric and electro-optic properties. Ferroelectric thin films have received considerable attention because of their use in non-volatile memory applications [ferroelectric random-access memories (FRAMs)] [1–3]. Extensive work has been reported on lead zirconium titanate (PZT), but one of the problems with PZT is its fatigue resistance. PZT tends to degrade most of the initial amount of switching charge after 10^6–10^8 cycles of full polarization switching [4]. More recently, bismuth oxide layered ferroelectric materials based on $SrBi_2Ta_2O_9$ (SBT), $SrBi_2Nb_2O_9$ (SBN) and their solid solutions have created the interest due to their excellent ferroelectric properties (high remnant polarization, P_r, and low coercive field, E_c) characterized by limited polarization fatigue up to 10^{12} cycles and a low leakage current [5–9].

Layered perovskite strontium bismuth tantalate, $SrBi_2Ta_2O_9$, is a member of the Aurivillius family having the general formula $(Bi_2O_2)^{2+}(A_{n-1}B_nO_{3n+1})^{2-}$, where A = Ca^{2+}, Ba^{2+}, Sr^{2+}, Bi^{2+}, etc.; B = Fe^{3+}, Ti^{4+}, Nb^{5+}, Ta^{5+}, W^{6+}, Mo^{6+}, etc., and n indicates the number of corner sharing octahedral forming the perovskite like slabs [10]. Most of the works reported on the improvement of the dielectric and ferroelectric properties are based on A-site substitutions [11–13]. For example, the replacement of Sr^{2+} ions by a smaller cation Ca^{2+} results in an increase in its dielectric constant and the Curie temperature, T_c [14]. However, there has not been any extensive study on the

* Corresponding author. Tel.: +91 11 30972376; fax: +91 11 27871023.
E-mail address: akj6467@indiatimes.com (A.K. Jha).

0272-8842/$30.00
doi:10.1016/j.ceramint.2005.07.013

dielectric properties of the layered perovskite, SBT, through B-site (Ta^{5+}) substitutions with other cations of higher oxidation state. We report here the effect of tungsten substitution for tantalum on the structural, dielectric and impedance properties of $SrBi_2Ta_2O_9$ ferroelectric ceramics.

2. Experimental

Samples of compositions $SrBi_2(W_xTa_{1-x})_2O_9$ (SBWT), with x ranging from 0.0 to 0.2 were synthesized using solid-state reaction method taking $SrCO_3$, Bi_2O_3, Ta_2O_5 and WO_3 (all from Aldrich) in their stoichiometric proportions. The powder mixtures were thoroughly ground and passed through sieve of appropriate size and then calcined at 900–1050 °C in air for 2 h. The calcined mixtures were ground and admixed with about 1–1.5 wt.% polyvinyl alcohol (Aldrich) as a binder and then pressed at ∼300 MPa into disk shaped pellets. The pellets were sintered at 1230 °C for 2 h in air. X-ray diffractograms of both the calcined and sintered samples were recorded using a Bruker diffractometer in the range $20^\circ \leq 2\theta \leq 60^\circ$ with Cu Kα radiation. The sintered pellets were polished to a thickness of ∼1 mm, coated with silver paste on both the sides for use as electrodes, and finally heated at 550 °C for 1/2 h. The dielectric and impedance measurements were carried out using a Solartron-1260 impedance/gain-phase analyzer operating at oscillation amplitude of 1 V. Dielectric constant as a function of temperature was measured at a frequency of 100 kHz while the impedance measurements were carried out in the frequency range of 10–10^6 Hz.

3. Results and discussion

3.1. XRD analysis

Fig. 1 shows the XRD patterns of the various SBWT sintered samples with all the characteristic peaks of the layered perovskite phase. It is observed that the single phase layered perovskite structure is obtained in the range $0.0 \leq x \leq 0.05$. For samples with $x > 0.05$ an unidentified peak is also observed. Since the intensity of this unidentified peak increases slightly with the increase of tungsten content, it might indicate the presence of tungsten at the interstitial sites. Lattice parameters of the samples as deduced from the X-ray diffractograms and refined using least square refinement method by a computer program package—Powdin [15]—are listed in the Table 1. On the basis of ionic radii of atoms and coordination number (Table 1) tungsten is expected to substitute at the tantalum (B) sites. A decrease in the lattice constants is expected due to a smaller ionic radius of W^{6+} than that of Ta^{5+}. The lattice parameters a and b, however, show negligible change with an increasing tungsten content up to $x = 0.05$. Further increase in tungsten content results in decrease of these parameters. Such

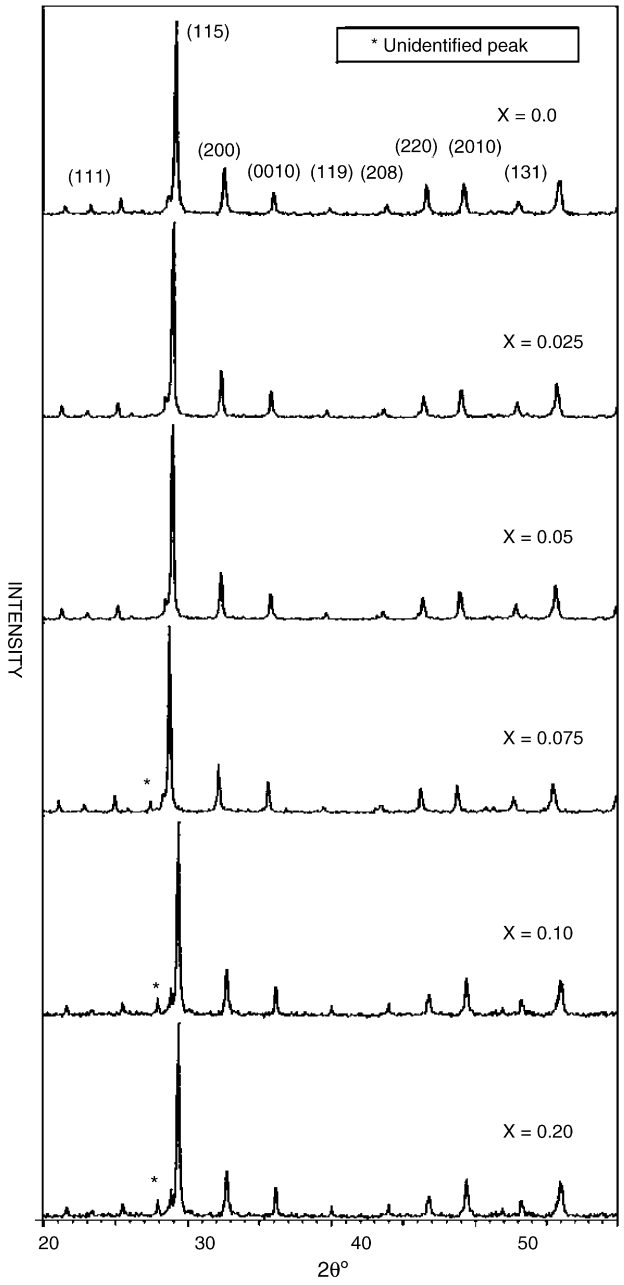

Fig. 1. XRD patterns of $SrBi_2(W_xTa_{1-x})_2O_9$ samples sintered at 1230 °C.

Table 1
Elements in most stable valence state with their ionic radius (IR) [18] and coordination number (CN)

Ions	IR (Å)	CN	x	a (Å)	b (Å)	c (Å)
Sr^{2+}	1.44	12	0.0	5.5146	5.5246	24.9017
Bi^{3+}	0.96	5	0.025	5.5232	5.5423	25.0678
Ta^{5+}	0.64	6	0.050	5.5214	5.5461	25.2366
W^{6+}	0.60	6	0.075	5.4851	5.5059	24.8525
			0.100	5.4785	5.4972	24.6670
			0.200	5.4786	5.4955	24.6595

Lattice parameters a–c of $SrBi_2(W_xTa_{1-x})_2O_9$ ceramics.

dependence of the parameters a and b on the tungsten content can be understood on the basis of the limited structural constraint imposed by the $[Bi_2O_2]^{2+}$ interlayer. It is known that in the layered perovskite structure $[Bi_2O_2]^{2+}$ interlayer imposes a constraint for structural relaxation [16]. When the concentration of tungsten is low, although the W^{6+} is smaller than Ta^{5+}, the structural constraint imposed from $[Bi_2O_2]^{2+}$ interlayer prevents the shrinkage of the crystal lattice [17]. However, for higher tungsten concentration, the shrinking tendency of the crystal lattice overcomes such limited structural constraint. Therefore, the lattice constants a and b decrease for higher concentration of tungsten. Changes observed in the lattice parameter c might be ascribed to the fact that the variation along the c–axis would be less constrained by the $[Bi_2O_2]^{2+}$ interlayer [17].

3.2. Dielectric properties

Fig. 2 illustrates the room temperature dielectric constant [Fig. 2(a)] and dielectric loss [Fig. 2(b)] of the sintered

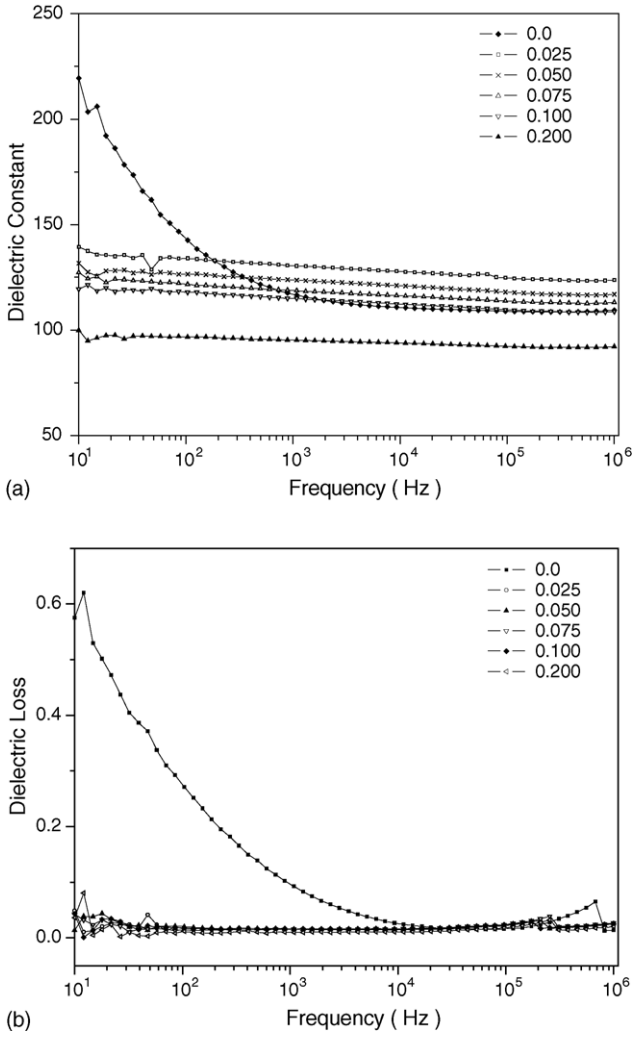

Fig. 2. (a) Dielectric constant and (b) dielectric loss of $SrBi_2(W_xTa_{1-x})_2O_9$ samples as a function of frequency measured at room temperature.

$SrBi_2(W_xTa_{1-x})_2O_9$ samples as a function of frequency in the range 10 Hz–1 MHz. In Fig. 2(a), the dielectric constant of undoped SBT sample shows a decrease as the frequency increases from 10 Hz to 1 kHz and remains constant at frequencies above 1 kHz. In contrast, dielectric constants of the doped samples, however, remain nearly invariant throughout the frequency range under study.

The dielectric constant (ε_r) of a material has four polarization contributions: electronic polarization (ε_e); ionic polarization (ε_i); dipolar polarization (ε_d) and space charge polarization (ε_s) [19]. Under the current experimental conditions (1 V and 10 Hz–1 MHz), contribution from the dipolar polarization is not expected as the electric field (1 V/cm) is too small to alter the orientation of the dipoles. Response frequencies for electronic and ionic polarizations are $\sim 10^{16}$ and 10^{13} Hz, respectively; and at frequencies above 1 kHz, contribution from space charge polarization is not expected [19]. It is known that the pristine $SrBi_2Ta_2O_9$ is not perfectly stoichiometric, but contains a certain amount of inherent defects (e.g. oxygen vacancies) resulting from the volatilization of Bi_2O_3 at high temperatures [20]. Such oxygen vacancies would act as space charge [21]. The high value of dielectric constant for low frequencies in case of undoped SBT can thus be attributed to the presence of such space charges. A negligible change of dielectric constant as frequency increases from 10 Hz to 1 MHz in the case of doped SBT ceramics implies that there is no appreciable contribution of space charge. It is possibly due to the compensation for the defects when B-site is substituted by higher valent cation. Because of the constraint of maintaining overall charge neutrality of the structure, substitution of W^{6+} ions for Ta^{5+} in the SBT should result in the formation of cation vacancies at A-sites. For substitution of two W^{6+} ions, one A-site (Sr site) should remain vacant. The corresponding defect representation can be expressed as:

$$\text{Null} = W_{Ta}^{\bullet} + \tfrac{1}{2}V''_{Sr} \quad (1)$$

where V_{Sr} denotes the Sr-vacant site. It is possibly due to the formation of cationic vacancies that effectively suppresses the formation of oxygen vacancies, which would eventually decrease the contribution of such space charges. The observed decrease in the room temperature dielectric constant with doping concentration [Fig. 2(a)] can be attributed to the smaller ionic radius of W^{6+}. This will result in a reduced electronic polarization and thereby cause a decrease in the room temperature dielectric constant with tungsten content. In Fig. 2(b), a steep decrease in the dielectric loss of undoped SBT ceramic is observed while dielectric loss of the tungsten doped SBT ceramics remained almost constant throughout the frequency range. The source of dielectric loss in insulating ceramics is space charge polarization and/or domain wall relaxation. Following the above discussion it is reasonable to believe that the space charge is primarily responsible for an appreciable increase in dielectric loss

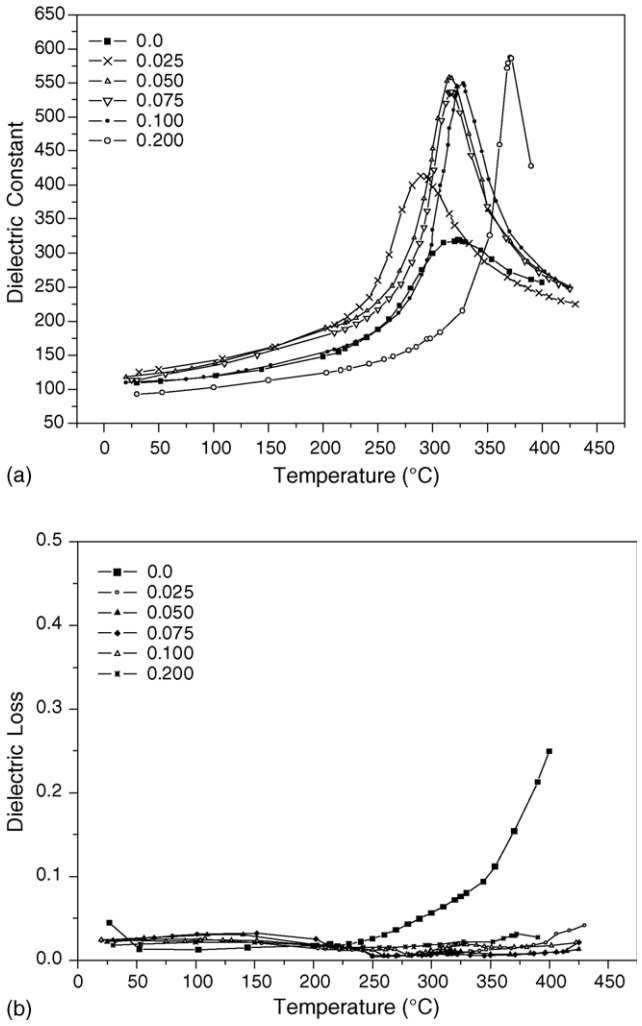

Fig. 3. (a) Dielectric constant and (b) dielectric loss of $SrBi_2(W_xTa_{1-x})_2O_9$ samples as a function of temperature at 100 kHz.

of undoped SBT ceramic. Possible formation of cationic vacancies on adding tungsten reduces the space charge and thus would result in decreasing the dielectric loss of doped $SrBi_2Ta_2O_9$ samples [21,22].

Dielectric constants and dielectric loss for doped and undoped ceramics as a function of temperature, measured at a frequency of 100 kHz with an oscillating amplitude of 1 V are depicted in Fig. 3(a) and (b), respectively. All the samples exhibit sharp transition in dielectric constant at their respective Curie temperatures (T_c). T_c decreases from 320 °C (for $x = 0.0$) to 291 °C (for $x = 0.025$) and shows an increasing trend over the composition range of $x = 0.05$–0.20. In isotropic perovskite ferroelectrics, doping at B-site (located inside an oxygen octahedron) with smaller ions results in increasing both the polarizability and Curie temperature due to "a large rattling space" available for the cations at B-sites [16]. In layered-structure perovskite, the crystal structure may not change as freely as that of isotropic perovskites with doping due to the structural constraint imposed by the $[Bi_2O_2]^{2+}$ interlayer. When the dopant

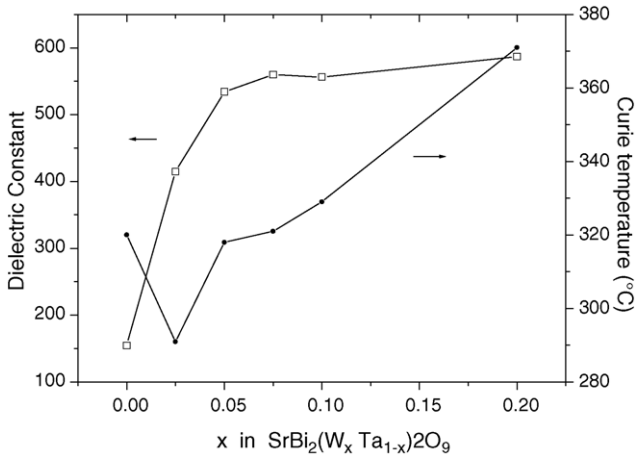

Fig. 4. The variation of Curie temperature and dielectric constant at T_c vs. concentration of tungsten in $SrBi_2(W_xTa_{1-x})_2O_9$ samples. The solid lines drawn are only for clarity.

concentration is low, both the lattice structure and the cation vacancies at the A-site possibly have resulted in an increased stress value. In such a situation the perovskite structure would be less stable and would cause a decrease in T_c. For higher W concentrations, decrease in the unit cell volume and the generation of cationic vacancies at the A-site lead to an enhancement of structural distortion and an eventual increase in T_c value [17]. Fig. 3(b) shows the dielectric loss (at 100 kHz) as a function of temperature for W-doped SBT. The observed reduction in the dielectric loss with W-doping may be related to the formation of cationic vacancies that effectively suppress the formation of oxygen vacancies.

In Fig. 4, it is observed that the peak dielectric constant at T_c increases with the doping concentration. For doping content between $x = 0.025$ to 0.05, the combined effect of nearly invariant lattice constants (or unit cell volume) and reduced ionic radius (W^{6+} in place of Ta^{5+}) would result in an increase of ionic polarization and hence the dielectric constant. Such an increase in dielectric constant indicates that the increase in ionic polarization is predominant over the decrease in electronic polarization corresponding to smaller ionic radius of W^{6+} than Ta^{5+}. It is known that the shift in T_c to higher temperatures corresponds to an increased polarizability, which can be explained well by the enlarged "rattling space" [23]. In addition, incorporation of tungsten ions into the SBT structure is likely to introduce some cationic vacancies for maintaining the electrical neutrality. These cationic vacancies make the domain motion easier and increase the dielectric permittivity [22,24] which would explain the observed increase in the dielectric constant.

3.3. Impedance spectroscopy

Complex impedance spectroscopy (CIS) is a well-known and powerful technique for investigating the electrical and dielectric properties of materials [25]. The ac technique of CIS enables us to evaluate and separate the contribution to

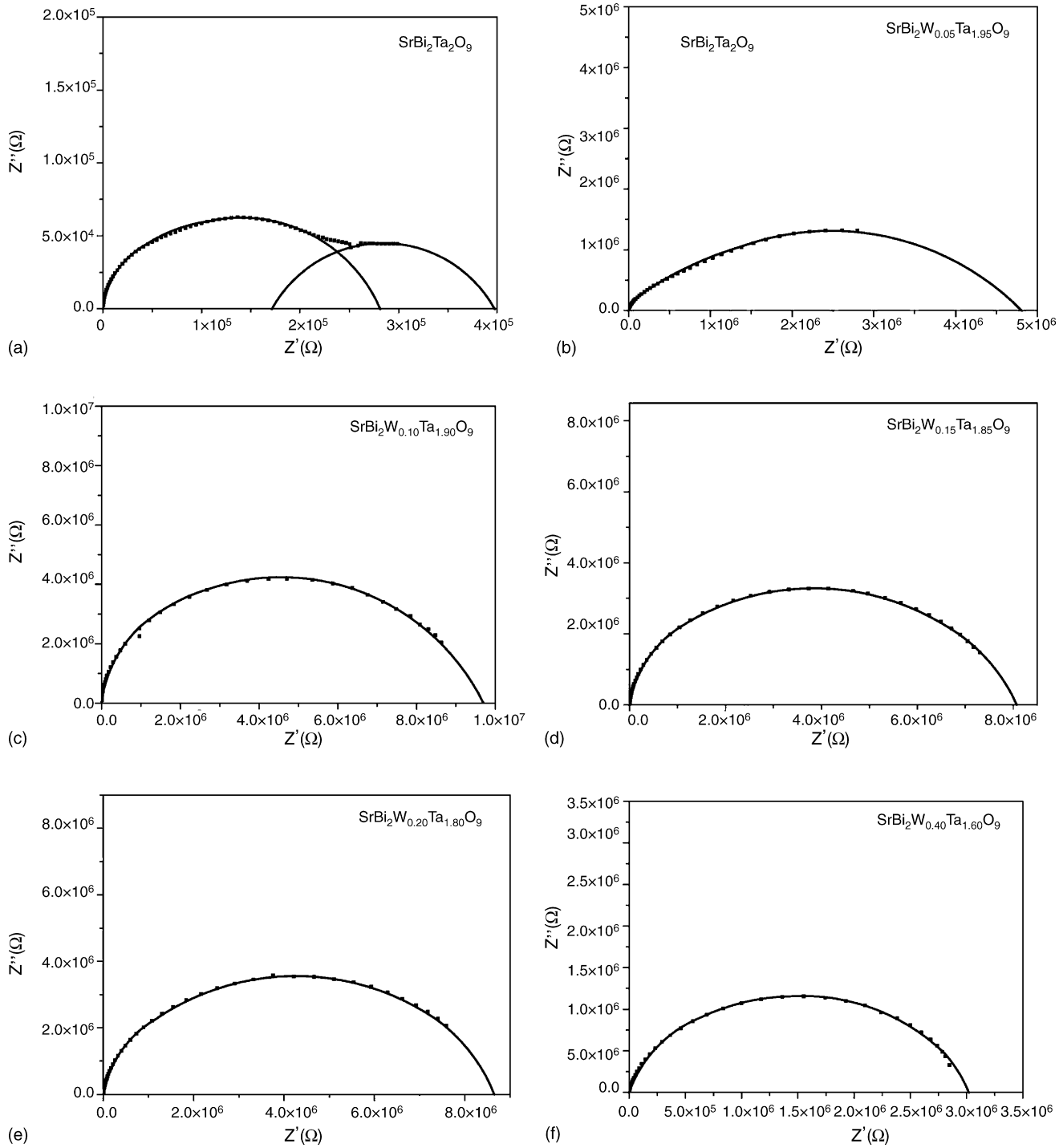

Fig. 5. Complex impedance plane plots at 430 °C for (a) $x = 0.0$, (b) $x = 0.025$, (c) $x = 0.050$, (d) $x = 0.075$, (e) $x = 0.10$, and (f) $x = 0.20$ in $SrBi_2(W_xTa_{1-x})_2O_9$.

the overall electrical properties, due to various components such as bulk, grain-boundary or polarization phenomenon in a material, in the frequency or time domain [26]. It is based on the principle of analyzing the ac response of a sample to a sinusoidal electrical signal and subsequent calculation of the resulting transfer function (impedance) with respect to the frequency of the applied signal. The electrical response recorded at the output, when compared with the sinusoidal input signal applied across the sample, provide us the impedance modulus $|Z|$ and phase shift (θ). The experimental output response so obtained, when depicted in a complex plane plot, appears in the form of a succession of semicircles/arcs in the frequency domain arising as a result of the contribution to the electrical properties due to various components such as the bulk material, grain boundary effects and interfacial polarization phenomenon (at the

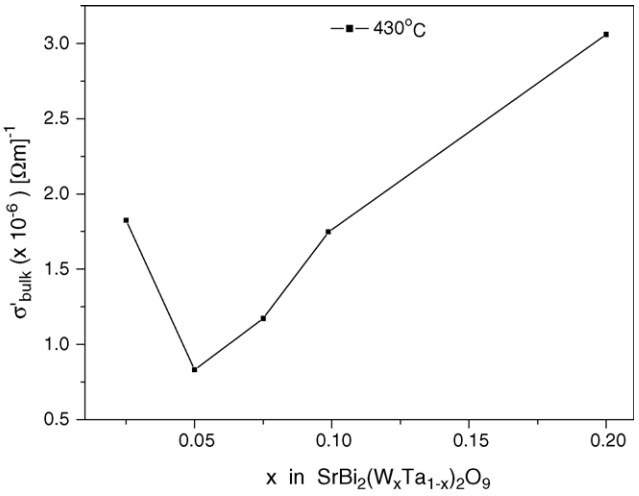

Fig. 6. Bulk (grain) conductivity, σ'_{bulk}, at 430 °C as a function of x in $SrBi_2(W_xTa_{1-x})_2O_9$.

material–electrode interface). The intersection of the first semicircle with the real-axis represents the bulk contribution (grain) to the real part of impedance, which can be used to derive the bulk conductivity according to the following equation [25]:

$$\sigma'_{bulk} = \frac{1}{\rho'} = \frac{1}{Z'}\left(\frac{t}{A}\right) \quad (2)$$

where σ'_{bulk} is the bulk conductivity, Z' is the real part of the impedance (intersection of semicircle on the real-axis), t is the thickness and A is the area of the sample.

Fig. 5 shows the complex impedance plane plots of the $SrBi_2(W_xTa_{1-x})_2O_9$ ceramics at 430 °C. For the undoped SBT, Z' versus Z'' curve is composed of two semicircles, a large one and a small one [Fig. 5(a)]. The large semicircle at high frequencies indicates the effect of the grain and the small one at low frequencies reflects the grain boundary effect. The Z'–Z'' plots of doped SBT samples are predominated by a single semicircle. The predominant semicircle represents the impedance contribution of the grains indicating that the grain boundaries in the case of doped SBT ceramics have a less significant contribution to the impedance.

Fig. 6 depicts the bulk conductivity (at 430 °C) calculated using Eq. (2) for different doping concentrations. The bulk conductivity of undoped SBT is found to be $2.95 \times 10^{-5}\ (\Omega m)^{-1}$ which decreases with increase in tungsten content up to $x = 0.05$ and increases for higher x values. In this system, oxygen vacancies act as ionic charge carriers [27]. The decrease of the bulk conductivity suggests that the introduction of cationic vacancies would suppress the formation of oxygen vacancies and, thus, decreases the conductivity [28]. Solubility limit for tungsten in the SBT structure appears to be around $x = 0.05$ where the conductivity exhibits a minimum. When $x > 0.05$, tungsten incorporation into SBT lattice is inhibited and the excess of tungsten manifests itself in the form of interstitial ions (also corroborated by the XRD observations), contributing to the electrical conduction as observed.

4. Conclusions

Tungsten doped $SrBi_2(W_xTa_{1-x})_2O_9$ $(0.0 \leq x \leq 0.20)$ ceramics synthesized by the solid state reaction route have been studied for their structural, dielectric and electrical properties. X-ray diffractograms of the samples reveal the single phase layered perovskite structure formation with tungsten content $x \leq 0.05$ with no detectable secondary phase. Measurements of dielectric constant (ε) and dielectric loss ($\tan\delta$) as a function of the temperature reveal a decrease in the Curie temperature (T_c) from 320 °C (for $x = 0.0$) to 291 °C (for $x = 0.025$) and an increasing trend over the doping range of $0.05 \leq x \leq 0.20$. The significant reduction in the dielectric loss have been considered in the light of suppression of oxygen vacancies by the cationic vacancies created by tungsten doping and the ensuing depletion of space charge. The increase in dielectric constant of the doped samples at their respective Curie temperatures with tungsten addition have been viewed in terms of a competition between the ionic and electronic polarizations. Bulk conductivity of the samples as deduced through ac impedance investigations indicates an increased electronic conduction beyond the observed solubility limit of 0.05 of tungsten doping.

Acknowledgments

The authors sincerely thank Dr. B.P. Singh and Dr. S.K. Singhal of the National Physical Laboratory, New Delhi, India for providing the dielectric and impedance measurements facilities. One of us (IC) is grateful to the University Grants Commission, New Delhi, India for the award of a Junior Research Fellowship.

References

[1] S.B. Desu, D.P. Vijay, *c*-Axis oriented ferroelectric $SrBi_2(Ta_xNb_{2-x})O_9$ thin films, Mater. Sci. Eng. B 32 (1995) 83–88.
[2] R.E. Jones Jr., P.D. Maniar, R. Moazzami, P. Zurcher, J.Z. Witowski, Y.T. Lii, P. Chu, S.J. Gillespie, Ferroelectric non-volatile memories for low-voltage, low power applications, Thin Solid Films 270 (1995) 584–588.
[3] J.F. Scott, C.A. Paz de Araujo, Ferroelectric memories, Science 246 (1989) 1400–1405.
[4] H. Watanabe, T. Mihara, H. Yoshimori, C.A. Paz de Araujo, Preparation of ferroelectric thin films of bismuth layer structured compounds, Jpn. J. Appl. Phys. 34 (1995) 5240–5244.
[5] C.A.P. De Araujo, J.D. Cuchlaro, L.D. McMillan, M.C. Scott, J.F. Scott, Fatigue-free ferroelectric capacitors with platinum electrodes, Nature 374 (1995) 627–629.

[6] M. Nagata, D.P. Vijay, X. Zhang, S.B. Desu, Formation and properties of $SrBi_2Ta_2O_9$ thin films, Phys. Status Solidi A 157 (1996) 75–82.
[7] I.S. Zheludev, Physics of Crystalline Dielectrics, Electrical Properties, vol. 2, Plenum Press, New York, 1971, pp. 474.
[8] V. Shrivastava, A.K. Jha, R.G. Mendiratta, Structural distortion and phase transition studies of Aurivillius type $Sr_{1-x}Pb_xBi_2Nb_2O_9$ ferroelctric ceramics, Solid State Commun. 133 (2004) 125–129.
[9] R. Jain, V. Gupta, K. Sreenivas, Sintering characteristics and properties of sol-gel derived $Sr_{0.8}Bi_{2.4}Ta_2O_9$, Mater. Sci. Eng. B78 (2000) 63–69.
[10] B. Aurivillius, Mixed bismuth oxides with layer lattices, Ark. Kemi. 1 (1949) 463–470.
[11] Y. Shimakawa, Y. Kubo, Y. Nakagawa, T. Kamiyama, H. Asano, F. Izumi, Crystal structures and ferroelectric properties of $SrBi_2Ta_2O_9$ and $Sr_{0.8}Bi_{2.2}Ta_2O_9$, Appl. Phys. Lett. 74 (1999) 1904–1906.
[12] J.K. Lee, B. Park, K.S. Hong, Effect of excess Bi_2O_3 on the ferroelectric properties of $SrBi_2Ta_2O_9$ ceramics, J. Appl. Phys. 88 (2000) 2825–2829.
[13] I. Coondoo, A.K. Jha, S.K. Agarwal, N.C. Soni, Effect of tungsten doping on the structural and dielectric behaviour of ferroelectric $SrBi_2Ta_2O_9$ ceramics, in: Proceedings of the XIII National Seminar on Ferroelectrics and Dielectrics, 2004, pp. 191–194.
[14] Y. Shimakawa, Y. Kubo, Y. Nakagawa, T. Kamiyama, H. Asano, F. Izumi, Crystal structure and ferroelectric properties of $ABi_2Ta_2O_9$ (A = Ca, Sr and Ba), Phys. Rev. B61 (2000) 6559–6563.
[15] E. Wu, POWD, an interactive powder diffraction data interpretation and indexing program Ver2.1, School of Physical Science, Flinders University of South Australia, Bedford Park, SA, JO42AU.
[16] Y. Wu, G. Cao, Ferroelectric and dielectric properties of strontium bismuth niobate vandates, J. Mater. Res. 15 (2000) 1583–1590.
[17] Y. Wu, C. Nguyen, S. Seraji, M.J. Forbess, S.J. Limmer, T. Chou, G. Cao, Processing and properties of strontium bismuth vandate niobate ferroelectric ceramics, J. Am. Ceram. Soc. 84 (2001) 2882–2888.
[18] R.D. Shannon, C.T. Prewitt, Effective ionic radii in oxides and fluorides, Acta Crystallogr. B25 (1965) 925–946.
[19] Relva C. Buchanan, Ceramic Materials for Electronics Processing, Properties and Applications, Marcel Dekker Inc., New York, 1986.
[20] B.H. Park, S.J. Hyun, S.D. Bu, T.W. Noh, J. Lee, H.D. Kim, T.H. Kim, W. Jo, Differences in nature of defects between $SrBi_2Ta_2O_9$ and $Bi_4Ti_3O_{12}$, Appl. Phys. Lett. 74 (1999) 1907–1909.
[21] Y. Noguchi, M. Miyayama, Large remanent polarization of vanadium-doped $Bi_4Ti_3O_{12}$, Appl. Phys. Lett. 78 (2001) 1903–1905.
[22] Y. Wu, S.J. Limmer, T.P. Chou, C. Nguyen, G. Cao, Influence of tungsten doping on dielectric properties of strontium bismuth niobate ferroelectric ceramics, J. Mater. Sci. Lett. 21 (2002) 947–949.
[23] K. Singh, D.K. Bopardikar, D.V. Atkare, A compendum of $T_c - P_s$ and $P_s - \Delta z$ data for displacive ferroelctrics, Ferroelectrics 82 (1988) 55–67.
[24] S. Takahashi, M. Takahashi, Effects of impurities on the mechanical quality factor of Lead Zirconate Titanate ceramics, Jpn. J. Appl. Phys. 11 (1972) 31–35.
[25] J.R. MacDonald, Impedance Spectroscopy, New York, Wiley, 1987.
[26] T.C. Chen, C.L. Thio, S.B. Desu, Impedance spectroscopy of $SrBi_2Ta_2O_9$ and $SrBi_2Nb_2O_9$ ceramics correlation with fatigue behavior, J. Mater. Res. 12 (1997) 2628–2637.
[27] B. Angadi, P. Victor, V.M. Jali, M.T. Lagare, R. Kumar, S.B. Krupanidhi, Ac conductivity studies on the Li irradiated PZT and SBT ferroelectric thin films, Mater. Sci. Eng. B100 (2003) 93–101.
[28] H.S. Shulman, M. Testorf, D. Damjanovic, N. Setter, Microstructure, electrical conductivity, and piezoelectric properties of bismuth titanate, J. Am. Ceram. Soc. 79 (1996) 3124–3128.